

# INNOVATIVE SUPERSONIC TRANSPORT CONFIGURATION BY BIPLANE WING / TWIN-BODY FUSELAGE

Wataru YAMAZAKI\*, Kazuhiro KUSUNOSE\*\*

\*Associate Professor, Nagaoka University of Technology, Japan

\*\*Visiting Research Scientist, Japan Aerospace Exploration Agency, Japan

**Keywords:** SST, Twin-Body Fuselage, Biplane Wing, Shock Wave, Sonic Boom

## Abstract

*A biplane wing / twin-body fuselage configuration is discussed for next-generation supersonic transport configuration. Its aerodynamic performance as well as sonic boom performance is investigated by using numerical approaches in this study. Thanks to the successful interactions of shock waves between the biplane wing as well as the twin-body fuselages, remarkable drag reduction and better sonic boom performance have been achieved at our design Mach number of 1.7. The superiority of the proposed SST configuration over conventional configurations is clearly demonstrated.*

## 1 Introduction

A fundamental problem preventing large commercial aircraft from supersonic flight is the creation of strong shock waves, whose effects are felt at the ground in the form of sonic booms. Since the poor fuel efficiency as well as the sonic boom noise at supersonic flight is mainly due to the effect of strong shock waves, the reduction of shock strength is very important to realize low-drag / low-boom supersonic transport (SST) configurations. A reduction method of the shock strength due to the lifted wing has been discussed in literature [1-4] by introducing a supersonic biplane wing concept. In this concept, the strength of wave drag has been successfully reduced by the interference of shock waves between the biplane. According to Ref.[1], the wave drag at zero lift of the biplane airfoil was reduced by nearly 90% compared to

an equal volume diamond-wedge airfoil in two dimensional inviscid simulations.

Inspired by the supersonic biplane wing concept, a twin-body fuselage concept has also been proposed by the present authors for more advanced SST configurations [5-6]. A same kind of twin-fuselage concept has been investigated in Ref.[7] in which fundamental wind tunnel experiments have been performed at Mach number of 2.7. The main purpose of our concept of the twin-body fuselage is to reduce the wave drag due to the volume of aircraft's fuselage. Furthermore, unnecessary wave interactions between the fuselages were minimized by using a shape optimization approach. According to Ref.[5], over 20% total drag reduction was achieved by the optimized twin-body fuselage compared with the Sears-Haack (SH) single-body fuselage under the constraint of fixed fuselage volume. The SH body [8] is well-known as the supersonic single-body configuration that has the lowest wave drag for specified volume and length.

The fusion of the two advanced concepts yields an innovative SST configuration which is a biplane wing / twin-body fuselage configuration. In this research, therefore, the wave drag characteristics as well as the sonic boom characteristics of the innovative SST configurations are investigated by utilizing computational fluid dynamics (CFD) approaches. The freestream Mach number ( $M_\infty$ ) in this study is set to our design Mach number of 1.7.

## 2 Computational Methodologies

In this section, the computational methodologies utilized in this research are concisely introduced.

### 2.1 CFD Approaches

Three-dimensional supersonic inviscid flows are analyzed by an unstructured mesh CFD solver of TAS (Tohoku University Aerodynamic Simulation)-code [9-10]. Compressible Euler equations are solved by a finite-volume cell-vertex scheme. The numerical flux normal to the control volume boundary is computed using the approximate Riemann solver of Harten-Lax-van Leer-Einfelds-Wada (HLLEW) [11]. The second-order spatial accuracy is achieved by the Unstructured MUSCL (U-MUSCL) approach [10,12] with Venkatakrishnan's limiter [13]. The LU-SGS implicit method for unstructured meshes [14] is used for the time integration. Three-dimensional unstructured meshes are generated using the TAS-mesh package, which includes surface mesh generation by an advancing front approach [15-16] and tetrahedral volume mesh generation by a Delaunay approach [17]. The high accuracy of this unstructured mesh CFD approach has already been confirmed in literature [10,18].

### 2.2 Sonic Boom Analysis

The sonic booms on the ground are predicted by a nonlinear acoustic propagation solver of Xnoise [19-20] which has been developed by Japan Aerospace Exploration Agency (JAXA). An augmented Burgers equation is numerically solved by using the operator split method, which takes into account the effects of nonlinearity, geometrical spreading, inhomogeneity of atmosphere, thermo-viscous attenuation and molecular vibration relaxation. In this approach, initial (input) pressure distributions are extracted from CFD solutions on the lower side of SST configurations (typically two fuselage lengths below). Then the propagation of the pressure distribution to the ground is solved by the augmented Burgers equation.

### 2.3 Skin Friction Drag Estimation

In this research, skin friction drags of various SST configurations are estimated by introducing simple algebraic skin friction models. Assuming that the boundary layer along the body is fully turbulent, the skin friction drag coefficient can be estimated as:

$$C_{Df} = C_f \frac{S_{wet}}{S_{ref}} \quad (1)$$

where  $C_f$  is the averaged turbulent skin friction coefficient on the wetted area of the body, and  $S_{wet}$  and  $S_{ref}$  are respectively the wetted area of the body and reference area. The skin friction coefficient for turbulent boundary layer conditions can be calculated by the following Prandtl-Schlichting flat-plate skin friction formula [21-23]:

$$C_f = \frac{0.455}{(\log_{10} Re)^{2.58} (1 + 0.144 M_\infty^2)^{0.65}} \quad (2)$$

where  $Re$  and  $M_\infty$  are respectively the Reynolds number and freestream Mach number. In this research, the Reynolds number is given at the cruise condition of Concorde (total length of 62[m]). Since the speed of sound ( $a_\infty$ ) and kinematic viscosity ( $\nu_\infty$ ) at the altitude of 18,000[m] are respectively 295.069[m/s] and  $1.1686 \times 10^{-4}$ [m<sup>2</sup>/s] according to Ref.[23], the Reynolds number for the fuselage body is calculated as:

$$Re = \frac{M_\infty a_\infty l}{\nu_\infty} \cong 266 \times 10^6 \quad (3)$$

The Reynolds number for the main wing is calculated in the same manner with its mean chord length. The skin friction drag coefficients of the fuselage and wing are separately estimated with the corresponding Reynolds numbers by using Eqs.(1-2). In Refs.[1,2,24], predicted friction drags based on the algebraic skin friction models are compared with those based on viscous CFD computations. It has been concluded that the simple algebraic skin friction models are reasonably accurate for the prediction of friction drag in supersonic flows.

### 2.4 Validation Study

The validity of the present computational approaches is concisely discussed in this subsection. The sonic booms generated from the N-wave model (NWM) and low-boom model (LBM) at  $M_\infty$  of 1.58-1.59 are discussed, that are the test cases of D-SEND#1 project of JAXA [25-26]. In its experiments, the sonic boom distributions were measured at about 3,500[m] away from the models. In this validation study, the CFD analyses are performed at the freestream Mach numbers to extract the initial pressure distributions as shown in Fig.1. Then the sonic boom propagations are solved to compare with the experimental sonic boom distributions, whose results are shown in Fig.2. The fluctuations of the experimental data in the range of  $0.03 < t < 0.05$ [s] are considered to be the effect of atmospheric turbulences. Qualitative agreements with the experimental data can be confirmed in the both NWM and LBM cases, which indicates the validity of the present computational methods.

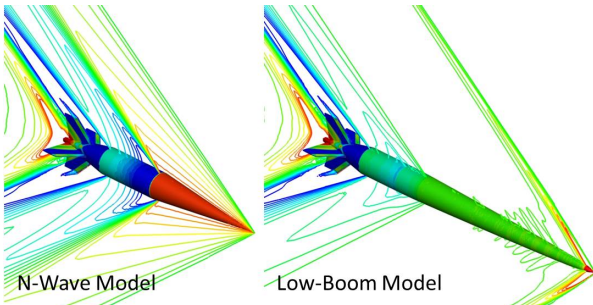


Fig.1 D-SEND#1 Experimental Models

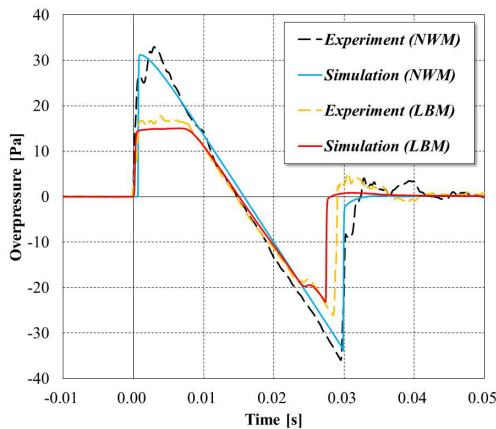


Fig.2 Comparison with Experimental Data of D-SEND#1 Project

### 3 Twin-Body Fuselage Concept

In this section, the supersonic twin-body fuselage concept [5] is briefly reviewed. According to Refs.[27-28], the supersonic wave drag due to the volume of an fuselage body is expressed as follows:

$$D_{wave\_vol} = qk \frac{V^2}{l^4} \quad (4)$$

where  $q$  and  $k$  are respectively the dynamic pressure and a constant. The wave drag due to the volume is proportional to the square of its volume  $V$  while it is inversely proportional to the fourth power of its length of aircraft  $l$ . The first approach to reduce the drag is to increase  $l$  while it is restricted by both operational and structural concerns. The other approach is to reduce  $V$  while it is also a difficult task for a large-sized SST. When both  $l$  and  $V$  are predetermined, it is well known that the SH body is the theoretical optimal configuration to minimize the wave drag.

Since the wave drag of the airplane's fuselage is proportional to the square of its volume when the body length is fixed, if we split a large single-body fuselage into two individual small bodies, the wave drag of each split body will reduce to 1/4 of that of the original one. The total drag of the twin-body configuration, then, becomes 1/2 of the original single-body fuselage under the constant-volume and constant-length conditions. This is the major point of view of the supersonic twin-body fuselage concept and is inspired by the wave reduction effect of the supersonic biplane airfoils. It is, however, important to note that this estimated wave drag for the twin-body configuration is reasonable only when the wave interactions between these individual bodies do not exist. In order to make a realistic airplane's fuselage, those two split bodies should be located reasonably close to each other. Therefore, unnecessary wave interactions between the bodies will always exist, resulting in an additional wave drag. To minimize the unnecessary wave interactions, the twin-body fuselage configuration was designed by using an optimization approach [29] with constraints of a fixed volume and fixed distance ratio between the twin bodies. As the result, a non-

axisymmetrical twin-body fuselage was proposed as the optimal configuration.

In Fig.3, the pressure contours around single/twin-body fuselage configurations are shown. These inviscid computations are performed at  $M_\infty$  of 1.7 and angle of attack ( $\alpha$ ) of 2 degrees. The aerodynamic performance of these configurations is summarized in Table 1. A same reference area is used in the all cases for the evaluation of all drag coefficients, which is the projected area of a main wing (it is defined in the next section). It is important to note that the all configurations have the same volume of fuselage in total. Although the twin-body configurations have larger skin friction drag than the single-body configuration, the total drag coefficients of them are lower than that of the single-body configuration. The optimal configuration has the lowest total drag among the four cases, which is about 23% lower than the single-body SH configuration. The non-axisymmetrical optimal shape is relatively flat at the inner side of the bodies. Since the wave interactions between bodies should be minimized with the cut SH twin-body configuration, it can be confirmed that the optimal configuration achieves successful wave interactions between the twin-bodies.

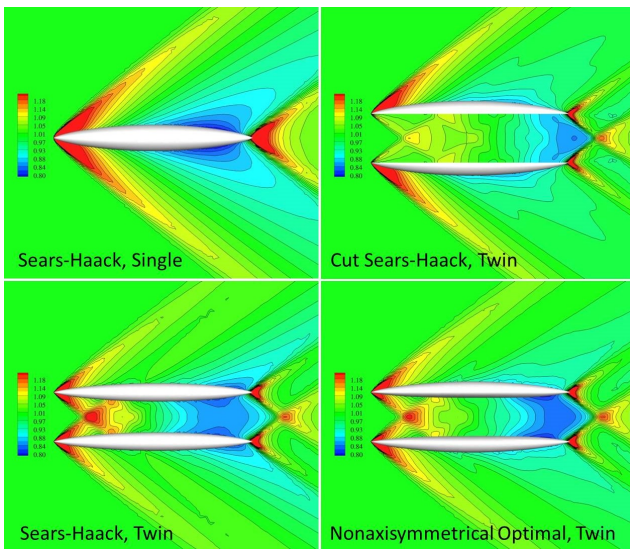


Fig.3 Pressure Contours around Single/Twin-Body Fuselage Configurations

Table 1 Aerodynamic Performance of Single/Twin-Body Fuselage Configurations

	Inviscid Drag	Friction Drag	Total Drag
SH, Single	215.0	42.8	257.9
SH, Twin	147.9	60.3	208.2
Cut SH, Twin	154.7	70.0	224.7
Optimal, Twin	135.9	61.5	197.4

(Drag coefficients in drag count, 1 drag count = 0.0001)

#### 4 Aerodynamic Performance of Wing-Body Configurations

In this section, the aerodynamic performance of biplane wing / twin-body fuselage SST configurations is discussed. Unswept tapered biplane wing configurations are designed for this research. The aspect and taper ratios are respectively set to about 7 and 0.25. The chord length of the main wing at the root section is about  $l/6$ . A vertical wingtip plate is arranged between the wings to increase the two-dimensionality of the flow around the biplane wing. For appropriate shock interactions, the vertical distance between the wings is shortened at the outer wing by adding a dihedral angle to the lower wing. The Busemann-type as well as Licher-type [30,1] biplane wing configurations are discussed in this research. The section airfoil thickness ratios of the Busemann-type biplane are set to 5% of the chord length in both the upper and lower wings. The thickness ratios of the Licher-type biplane (different between the upper/lower wings) are determined to have the same sectional area with the Busemann-type biplane wing. The mounting angle ( $\beta$  in Fig.4) of the Licher-type wing is set to 2 degrees. The outlines of the biplane wings are shown in Fig.4. For comparison purpose, an unswept tapered conventional wing configuration is also designed whose section shape is a diamond-wedge airfoil. The thickness ratio is set to 10%, which has the same volume as the biplane wing configurations. The outline of this wing is also included in Fig.4. These wings are respectively merged with the single and twin-body fuselages to make SST wing-body configurations. The trihedral figure of the wing-body configuration from the Busemann-type biplane wing and the optimal twin-body configuration is shown in

Fig.5. The following combinations are investigated in this research:

- SH single-body with diamond-wedge wing
- SH single-body with Busemann biplane wing
- SH twin-body with diamond-wedge wing
- SH twin-body with Busemann biplane wing
- Optimal twin-body with biplane wings

The unstructured mesh around a wing-body configuration is visualized in Fig.6.

In Figs.7-8, the pressure contours around the SST configurations are shown at the condition of  $M_\infty$  of 1.7 and lift coefficient ( $C_L$ ) of 0.15. We can observe (successful) shock interactions between the wings as well as the twin bodies. The inviscid drag polar curves of these configurations at  $M_\infty$  of 1.7 are shown in Fig.9. A same reference area is used in the all cases for the evaluation of lift/drag coefficients, which is the projected area of the main wing (same in the all wing configurations). It can be understood that the biplane wing concept and the twin-body fuselage concept respectively have individual drag reduction effects. We can summarize that about 150cts drag reduction was achieved by the adoption of the biplane wing configuration, and then separately, about 60~80cts another drag reduction was achieved by the adoption of the twin-body fuselage configuration. The best aerodynamic performance is achieved by the optimal twin-body fuselage configurations. In detail, the Licher biplane wing configuration has better aerodynamic performance than the Busemann biplane wing configuration at the conditions of  $C_L > 0.1$ .

The skin friction drag coefficients of the SST configurations are estimated by the algebraic model of Eqs.(1-2). The total (inviscid + skin friction) drag polar curves of these configurations at  $M_\infty$  of 1.7 are shown in Fig.10. Since the twin-body / biplane wing configurations have larger wetted areas than the single-body / diamond-wedge wing configurations, the drag reduction effect shortens by taking into account the viscous contributions. But the superiorities of the twin-body / biplane wing configurations can be still observed. The aerodynamic performance at  $M_\infty$  of 1.7 and  $C_L$  of 0.15 is summarized in Table 2.

Although the all configurations have the same volume of fuselage/wing, the optimal twin-body / Licher biplane wing configuration achieves a 38% total drag reduction compared with the SH single-body / diamond-wedge wing conventional configuration.

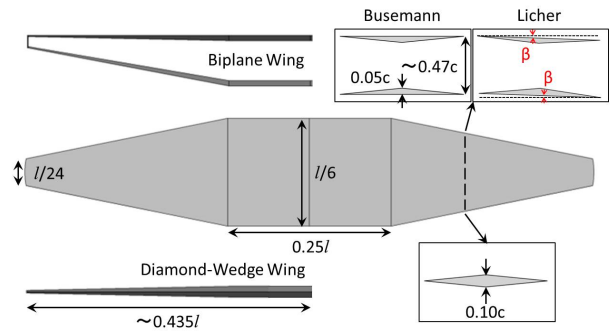


Fig.4 Outlines of Wing Configurations

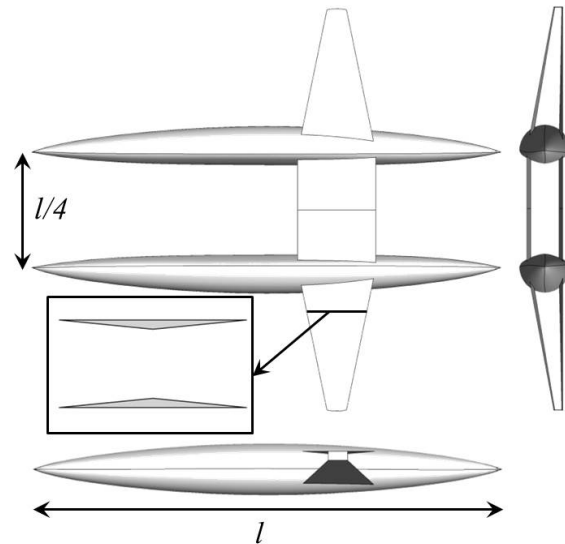


Fig.5 Trihedral Figure of a Twin-Body / Biplane Wing SST Configuration

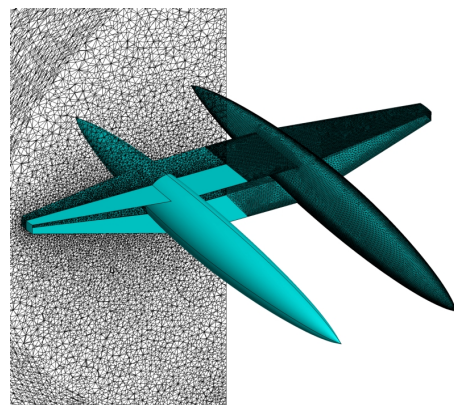


Fig.6 Unstructured Volume/Surface Mesh around SST Configuration

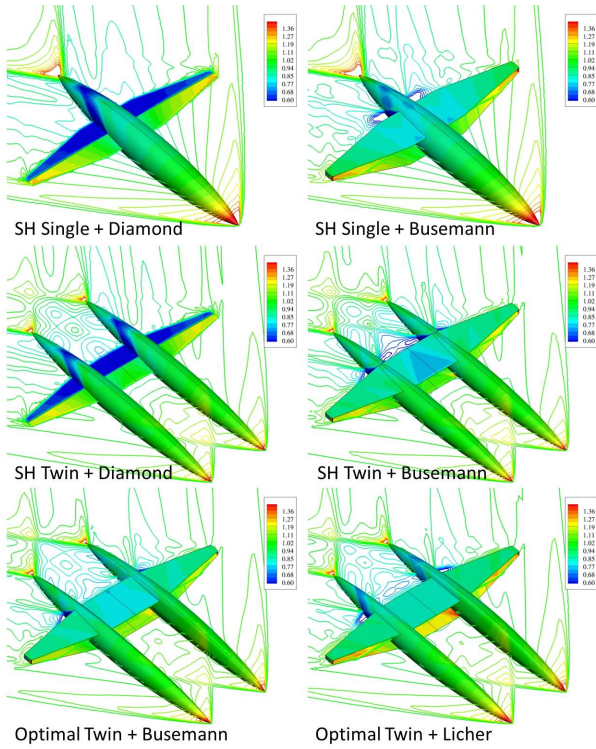


Fig.7 Pressure Contours around SST Configurations

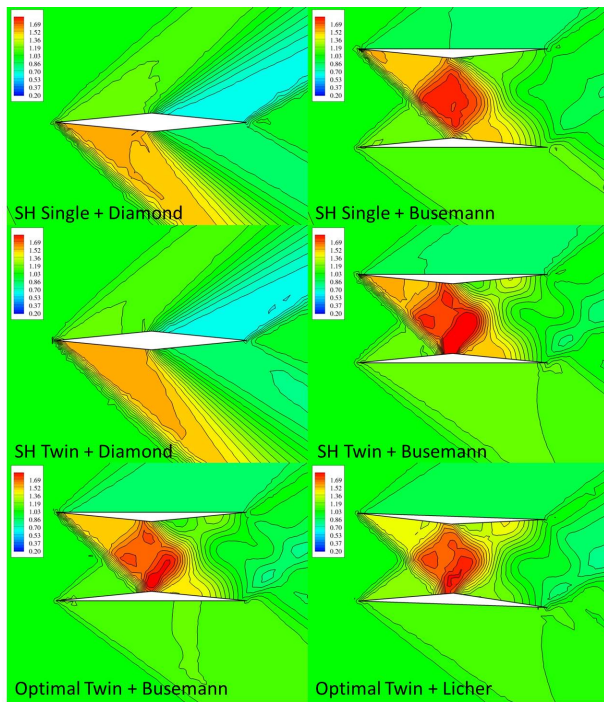


Fig.8 Pressure Contours at 60% semi-span Section of SST Configurations

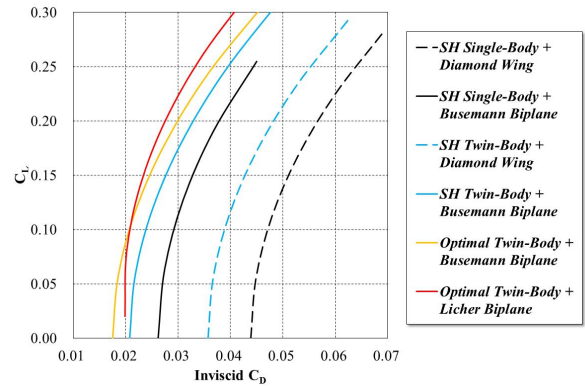


Fig.9 Inviscid Drag Polar at  $M_\infty$  of 1.7

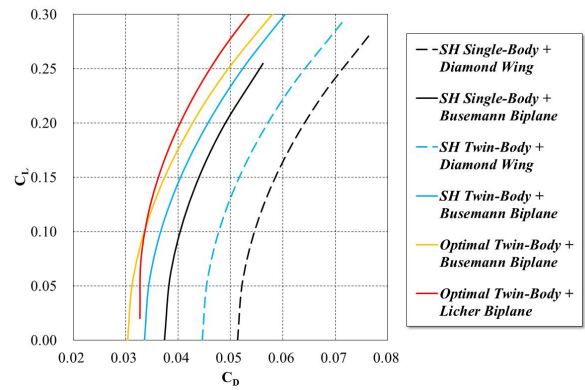


Fig.10 Total Drag Polar at  $M_\infty$  of 1.7

Table 2 Aerodynamic Performance of SST Configurations at  $M_\infty$  of 1.7 and  $C_L$  of 0.15

	$\alpha$ [deg]	Inviscid Drag	Friction Drag	Total Drag
SH Single + Diamond	2.66	511.8	74.8	586.7
SH Single + Busemann	2.35	328.4	112.1	440.5
SH Twin + Diamond	2.57	428.4	89.1	517.5
SH Twin + Busemann	2.47	276.7	128.1	404.8
Optimal Twin + Busemann	2.50	245.6	128.6	374.2
Optimal Twin + Licher	0.16	234.8	128.4	363.2

(Drag coefficients in drag count, 1 drag count = 0.0001)

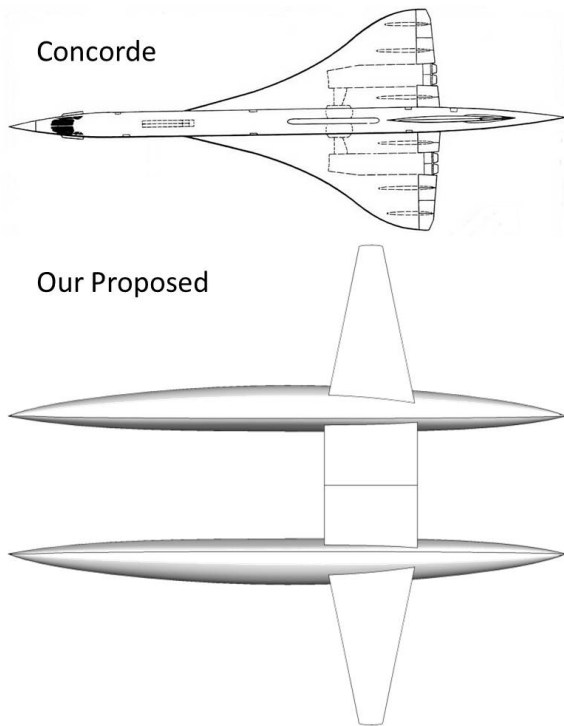


Fig.11 Comparison with Concorde at Same Fuselage Length

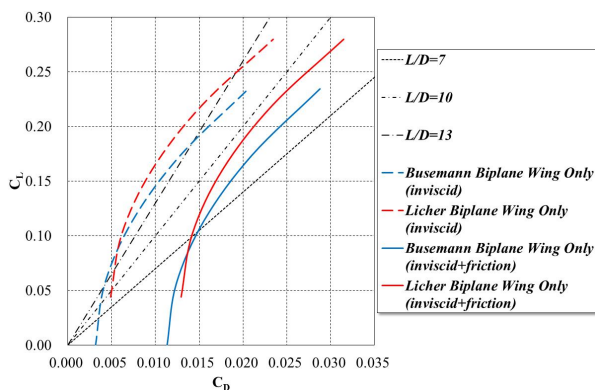


Fig.12 Drag Polar of Wing Only Configurations at  $M_\infty$  of 1.7

Readers may notice the low L/D value of the proposed SST configuration which is less than 5 while that of Concorde is known to be as about 7~8 (at  $M_\infty$  of 2.0). The one of the major reasons is its larger fuselage volume than Concorde. In Fig.11, the both configurations are compared with the same fuselage length. The fuselage volume of our proposed configuration is approximately four times more than that of Concorde, which yields the lower L/D value than Concorde in this study. The Busemann / Licher wing only configurations are also

analyzed at  $M_\infty$  of 1.7, whose results are shown in Fig.12. In the Licher wing only configuration, its L/D is over 9 even when taking into account the viscous effect. It is, therefore, confirmed that the proposed twin-body / biplane wing configuration is a promising candidate for the next-generation large-sized SST.

### 5 Sonic Boom Performance of Wing-Body Configurations

The sonic boom performance of the proposed SST configurations is also investigated at  $M_\infty$  of 1.7 and  $C_L$  of 0.15. In this study, the pressure distributions are extracted at two fuselage lengths lower from the SST configurations on the symmetry plane as is shown in Fig.13. In the sonic boom propagation analyses, standard atmosphere temperature/humidity profiles are utilized. The fuselage length and the cruise altitude are respectively set to 62[m] and 18,000[m], that are given from the conditions of Concorde.

The pressure distributions extracted at the line of Fig.13 are compared in Fig.14. Larger pressure variations can be observed in the diamond wedge wing configurations at the medium of the distributions. The distributions of “SH Twin + Busemann” and “Optimal Twin + Busemann” are almost equivalent. The propagations of the pressure distributions to the ground are respectively solved by the augmented Burgers equation, and then the pressure distributions on the ground are compared in Fig.15. The sonic boom characteristics can be primarily classified according to the wing configurations. The diamond wedge wing configurations have typical “N wave” distributions while the other configurations have two peaks in the distributions. The three Busemann biplane wing configurations have approximately the same distributions at the ground, which implies the insignificance of the fuselage body configurations to the sonic boom performance in this study. Three major sonic boom performance parameters of maximum pressure rise ( $\Delta P$ ), sound pressure level ( $L_P$ ) and impulse ( $Im$ ) are calculated from the pressure distributions on the ground and these parameters

are summarized in Table 3. The best sonic boom performance is obtained in the optimal twin-body fuselage with the Licher biplane wing, whose maximum pressure rise is 38% lower than the single-body / diamond wedge wing configuration. The difference of the sonic boom performance between the Busemann and Licher biplane wing configurations with the optimal twin-body fuselage is primarily due to the angle of attack. Since the Licher wing has the mounting angle of 2 degrees, the angle of attack is lower than that of the Busemann wing configuration as indicated in Table 2. Therefore, the apparent angle of attack for the optimal twin-body fuselage is different between the two configurations, which yields the large difference of the sonic boom performance. The sound pressure level of the optimal twin-body / Licher biplane wing configuration is not much more than 124 [dB SPL] while that of Concorde is known to be over 130 [dB SPL]. According to Ref.[31], the target value of  $\Delta P$  for next-generation low-boom SST is considered to be about 24 [Pa], i.e. 121.6[dB SPL]. For the proposition of more favorable next-generation SST configuration, therefore, not only the shock wave interactions between the body/wing, but also its detailed shape optimization minimizing sonic-boom will be required.

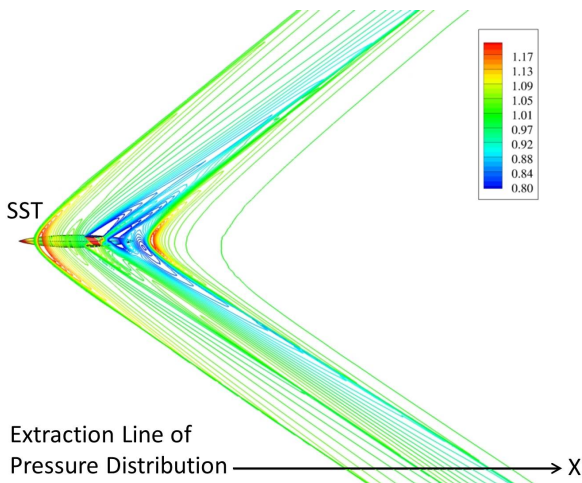


Fig.13 Extraction of Pressure Distribution for Sonic Boom Analysis

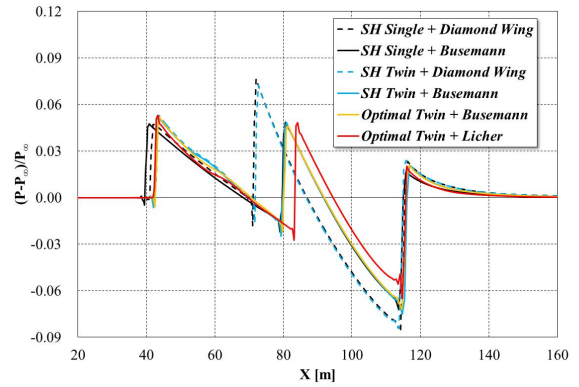


Fig.14 Pressure Distributions at Extraction Line

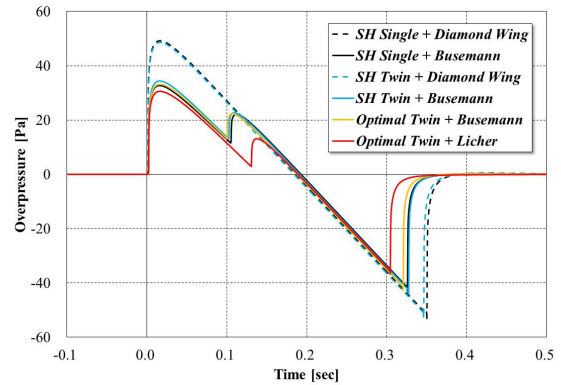


Fig.15 Pressure Distributions at Ground

Table 3 Sonic Boom Performance of SST Configurations at  $M_\infty$  of 1.7 and  $C_L$  of 0.15

	$\Delta P$ [Pa]	$L_p$ [dB SPL]	$Im$ [Pa·s]
SH Single + Diamond	<b>49.19</b>	<b>127.82</b>	<b>5.15</b>
SH Single + Busemann	<b>32.72</b>	<b>124.28</b>	<b>3.62</b>
SH Twin + Diamond	<b>48.58</b>	<b>127.71</b>	<b>5.04</b>
SH Twin + Busemann	<b>34.40</b>	<b>124.71</b>	<b>3.75</b>
Optimal Twin + Busemann	<b>33.18</b>	<b>124.40</b>	<b>3.61</b>
Optimal Twin + Licher	<b>30.59</b>	<b>123.69</b>	<b>2.95</b>

## 6 Concluding Remarks

In this research, twin-body fuselage / biplane wing configurations for a large-sized SST have been discussed. The wave drag characteristics / reduction by these innovative concepts have been discussed at our design freestream Mach number of 1.7 by using inviscid CFD computations. The increment of skin friction drag has also been discussed utilizing the standard algebraic (turbulent) skin friction models based on the wetted areas of SST configurations. Furthermore, the sonic boom performance of the innovative SST configurations has also been discussed. As one of the twin-body fuselage configurations, the non-axisymmetrical optimal configuration that we have designed beforehand was also investigated. As biplane wing configurations, Busemann / Licher type biplanes were investigated.

The biplane wing concept and the twin-body fuselage concept respectively have individual drag reduction effects. The combination of the optimal twin-body fuselage with the Licher biplane wing achieved the best aerodynamic performance among our investigated cases. The proposed SST configuration achieved a 38% total drag reduction compared with the single-body / diamond-wedge wing conventional configuration under constraints of fixed volume and fixed length of fuselage. This result indicates the remarkable aerodynamic superiority of our proposed optimal twin-body / biplane wing configuration.

The sonic boom characteristics of the SST configurations were primarily classified according to the wing configurations. The sonic boom performance parameters became better by the adoption of the biplane wing configurations. On the other hand, the fuselage body configurations had less effect to the sonic boom performance. The best sonic boom performance was also obtained in the optimal twin-body fuselage with the Licher biplane wing, whose maximum pressure rise at the ground is 38% lower than the single-body / diamond wedge wing conventional configuration.

For more sophisticated SST configuration, the design (optimization) of a wing/body fairing should be considered and the supersonic drag may be reduced more. Furthermore, low-boom design optimization will be also required for the proposition of more realistic low-boom / low-drag SST configurations. Since the fundamental availability of our proposed concept has been confirmed from the viewpoints of aerodynamics / sonic boom acoustics in this paper, we'll continue further development research studies to demonstrate its inclusive availability by additional multidisciplinary investigations.

## Acknowledgements

The authors are very grateful to Dr. Masashi KANAMORI, Dr. Yusuke NAKA, Dr. Yoshikazu MAKINO and Dr. Keiichi MURAKAMI of Japan Aerospace Exploration Agency (JAXA) for providing us their nonlinear acoustic propagation solver of Xnoise, as well as for their helpful advices. The authors also would like to thank Mr. Naohiko BAN of Nagaoka University of Technology for his help to make CAD models of SST configurations.

## References

- [1] Kusunose, K., Matsushima, K., and Maruyama, D., "Supersonic Biplane—A Review," Progress in Aerospace Sciences, Vol.47, pp.53-87, 2011.
- [2] Kusunose, K., Matsushima, K., Obayashi, S., Furukawa, T., Kuratani, N., Goto, Y., Maruyama, D., Yamashita, H., and Yonezawa, M., "Aerodynamic Design of Supersonic Biplane: Cutting Edge and Related Topics," The 21st century COE Program International COE of flow dynamics lecture series, Vol.5, Sendai, Tohoku University Press, 2007.
- [3] Matsushima, K., Kusunose, K., Maruyama, D., and Matsuzawa, T., "Numerical Design and Assessment of a Biplane as Future Supersonic Transport," Proceedings of the 25th ICAS Congress, ICAS Paper 2006-3.7.1, Hamburg, 2006.
- [4] Matsushima, K., Maruyama, D., Kusunose, K., and Noguchi, R., "Extension of Busemann Biplane Theory to Three Dimensional Wing Fuselage Configurations," Proceedings of the 27th ICAS Congress, ICAS Paper 2010-2.8.1, Nice, 2010.
- [5] Yamazaki, W., and Kusunose, K., "Aerodynamic Study of Twin-Body Fuselage Configuration for Supersonic Transport," Transactions of the Japan Society for Aeronautical and Space Sciences, Vol.56, No.4, pp.229-236, 2013.

- [6] Yamazaki, W., and Kusunose, K., "A Biplane Wing / Twin-Body Fuselage Configuration for Innovative Supersonic Transport," *Journal of Aircraft*, reviewing.
- [7] Wood, R. M., Miller, D. S., and Brentner, K. S., "Theoretical and Experimental Investigation of Supersonic Aerodynamic Characteristics of a Twin-Fuselage Concept," NASA-TP-2184, 1983.
- [8] Sears, W. R., "On Projectiles of Minimum Wave Drag," *Quarterly of Applied Mathematics*, Vol.4, No.4, pp.361-366, 1947.
- [9] Nakahashi, K., Ito, Y., and Togashi, F., "Some Challenges of Realistic Flow Simulations by Unstructured Grid CFD," *International Journal for Numerical Methods in Fluids*, Vol.43, No.6-7, pp.769-783, 2003.
- [10] Yamazaki, W., Matsushima, K., and Nakahashi, K., "Drag Prediction, Decomposition and Visualization in Unstructured Mesh CFD Solver of TAS-code," *International Journal for Numerical Methods in Fluids*, Vol.57, No.4, pp.417-436, 2008.
- [11] Obayashi, S., and Guruswamy, G. P., "Convergence Acceleration of a Navier-Stokes Solver for Efficient Static Aeroelastic Computations," *AIAA Journal*, Vol.33, No.6, pp.1134-1141, 1995.
- [12] Burg, C. O. E., "Higher Order Variable Extrapolation for Unstructured Finite Volume RANS Flow Solvers," *AIAA Paper 2005-4999*, 2005.
- [13] Venkatakrishnan, V., "On the Accuracy of Limiters and Convergence to Steady State Solutions," *AIAA Paper 93-0880*, 1993.
- [14] Sharov, D., and Nakahashi, K., "Reordering of Hybrid Unstructured Grids for Lower-Upper Symmetric Gauss-Seidel Computations," *AIAA Journal*, Vol.36, No.3, pp.484-486, 1998.
- [15] Ito, Y., and Nakahashi, K., "Direct Surface Triangulation Using Stereolithography Data," *AIAA Journal*, Vol.40, No.3, pp.490-496, 2002.
- [16] Ito, Y., and Nakahashi, K., "Surface Triangulation for Polygonal Models Based on CAD Data," *International Journal for Numerical Methods in Fluids*, Vol.39, Issue.1, pp.75-96, 2002.
- [17] Sharov, D., and Nakahashi, K., "Hybrid Prismatic/Tetrahedral Grid Generation for Viscous Flow Applications," *AIAA Journal*, Vol.36, No.2, pp.157-162, 1998.
- [18] Umeda, M., Takenaka, K., Hatanaka, K., Hirayama, D., Yamazaki, W., Matsushima, K., and Nakahashi, K., "Validation of CFD Capability for Supersonic Transport Analysis Using NEXST-1 Flight Test Results," *AIAA Paper 2007-4437*, 2007.
- [19] Yamamoto, M., Hashimoto, A., Takahashi, T., Kamamura, T., and Sakai, T., "Long-range Sonic Boom Prediction Considering Atmospheric Effects," *Proceedings of InterNoise 2011, Osaka*, 2011.
- [20] Yamamoto, M., Hashimoto, A., Takahashi, T., Kamakura, T., and Sakai, T., "Numerical Simulations for Sonic Boom Propagation through an Inhomogeneous Atmosphere with Winds," *AIP Conference Proceedings, Nonlinear Acoustics*, pp.339-342, 2012.
- [21] Raymer, D. P., "Aircraft Design: A Conceptual Approach Fourth Edition," *AIAA Education Series*, AIAA, 2006.
- [22] Krasnov, N. F., "Aerodynamics of Bodies of Revolution," Edited and Annotated by Morris, D. N., Elsevier, New York, 1970.
- [23] "Handbook of Aerospace Engineering: The Third Edition," The Japan Society for Aeronautical and Space Sciences, (eds.), Maruzen, 2005 (in Japanese).
- [24] Hu, R., "Supersonic Biplane Design via Adjoint Method," Dissertation for the degree of Doctor of Philosophy, Department of Aeronautics and Astronautics, Stanford University, 2009.
- [25] JAXA D-SEND Database Website, [http://d-send.jaxa.jp/d\\_send\\_1.html](http://d-send.jaxa.jp/d_send_1.html)
- [26] Naka, Y., "Sonic Boom Data from D-SEND#1," *JAXA-RM-11-010E*, 2012.
- [27] Jones, R. T., "Theoretical Determination of the Minimum Drag of Airfoils at Supersonic Speeds," *Journal of the Aeronautical Sciences*, Vol.19, No.12, pp.813-822, 1952.
- [28] Kroo, I., "Unconventional Configurations for Efficient Supersonic Flight," *VKI Lecture Series on Innovative Configurations and Advanced Concepts for Future Civil Aircraft*, 2005.
- [29] Yamazaki, W., and Mavriplis, D. J., "Derivative-Enhanced Variable Fidelity Surrogate Modeling for Aerodynamic Functions," *AIAA Journal*, Vol.51, No.1, pp.126-137, 2013.
- [30] Licher, R. M., "Optimum Two-Dimensional Multiplanes in Supersonic Flow," Report No. SM-18688, Douglas Aircraft Co., 1955.
- [31] Yoshida, K., "Low Sonic Boom Design Technology for Next Generation Supersonic Transport," *Journal of the Acoustical Society of Japan*, Vol.67, No.6, pp.245-250, 2011 (in Japanese).

### Contact Author Email Address

yamazaki@mech.nagaokaut.ac.jp

### Copyright Statement

The authors confirm that they, and/or their company or organization, hold copyright on all of the original material included in this paper. The authors also confirm that they have obtained permission, from the copyright holder of any third party material included in this paper, to publish it as part of their paper. The authors confirm that they give permission, or have obtained permission from the copyright holder of this paper, for the publication and distribution of this paper as part of the ICAS 2014 proceedings or as individual off-prints from the proceedings.